Liquid Crystals
Publication details, including instructions for authors and subscription information:
http://www.informaworld.com/smpp/title~content=t713926090

Estimation of microscopic rubbing alignment parameters

A. J. Pidduck[a]; G. P. Bryan-Brown[a]; S. D. Haslam[a]; R. Bannister[a]
[a] Defence Research Agency (DRA), Worcs., UK

To cite this Article Pidduck, A. J. , Bryan-Brown, G. P. , Haslam, S. D. and Bannister, R.(1996) 'Estimation of microscopic rubbing alignment parameters', Liquid Crystals, 21: 5, 759 — 763
To link to this Article: DOI: 10.1080/02678299608032889
URL: http://dx.doi.org/10.1080/02678299608032889

LIQUID CRYSTALS, 1996, VOL. 21, NO. 5, 759–763

Estimation of microscopic rubbing alignment parameters

by A. J. PIDDUCK*, G. P. BRYAN-BROWN, S. D. HASLAM
and R. BANNISTER
Defence Research Agency (DRA), St Andrews Road, Malvern,
Worcs. WR14 3PS, UK

(*Received 3 April 1996; in final form 17 June 1996; accepted 28 June 1996*)

We report an examination of the cloth-rubbing process, widely used to effect liquid crystal alignment, from a simplified microscopic perspective. We define strength of rubbing by the average applied force per rubbing fibre (approximately 11–22 μN under our conditions, assuming all fibres passing the surface make contact), and extent of rubbing by the fraction of total surface area contacted during the process. Fibre-surface microscopic contact widths estimated from atomic force microscopy images of rubbed alignment polymer surfaces were in the range 10–500 nm. Taking 100 nm as an average value, we show that the entire alignment surface may be contacted several times during a typical rubbing process. Fibre-surface contact shear stresses can approach the GPa range, several orders of magnitude greater than the macroscopic rubbing pressure.

Liquid crystal (LC) alignment in commercial nematic LC displays is widely achieved by the unidirectional cloth-rubbing of thin polymer films overlying the electrodes [1, 2]. The mechanics of the rubbing process have to date been defined by macroscopic parameters. Becker *et al.* [3] measured the work done per unit area during the rubbing process. Uchida *et al.* [4] proposed a rubbing strength parameter $RS = \gamma L$, where L is the length of cloth passing any given point on the surface during the rubbing process (the rubbing length) and γ is an undefined parameter related to rubbing pressure, fibre density and coefficient of friction. The rubbing is, however, intrinsically a microscopic process, involving mechanical interactions between individual rubbing fibres and the polymer surface. This is demonstrated particularly clearly by the rubbing-induced surface topographic features observed in recent atomic force microscopy (AFM) studies of polymer alignment layers [5–12]. In the present paper we therefore propose definitions for rubbing parameters from a microscopic perspective, and attempt their determination for our own experimental conditions. We use the average force per fibre F_f, as a measure of rubbing strength, and the 'rubbing ratio' (RR) of contacted to actual surface area, which is derived from estimates of the fibre-surface contact width w_f, as a measure of the extent or density of rubbing. If meaningful average values for F_f and w_f can be determined they provide the basis for a fundamental description of the fibre-surface contact mechanics, which may be helpful in identifying opportunities for improved control of the rubbing process. With this aim in mind, we also briefly discuss the relationship between F_f and w_f, and the stresses, temperatures and time scales occurring within the contact zone.

*Author for correspondence.

The macroscopic rubbing length parameter L, is defined for roller rubbing by [4, 13]:

$$L = N\ell(2\pi rv/60s \pm 1) \tag{1}$$

where r is the roller radius, ℓ is the length of cloth pressing against the substrate, v is the roller rotation rate (rpm), s is the substrate translation speed, and N is the total number of passes of the substrate by the roller; $\ell \approx (2r\delta)^{1/2}$, where δ is the maximum pile deformation. Seo [14] proposed a modified rubbing parameter as given by (1), but with ℓ replaced directly by δ. The equivalent microscopic parameter, n_f the number of fibres passing a position of unit width during rubbing, is given from the areal density of fibres in the rubbing cloth σ_f:

$$n_f = L\sigma_f \tag{2}$$

Assuming that all fibres within ℓ contact the surface, F_f is given by:

$$F_f = F_N/b\ell\sigma_f \tag{3}$$

where F_N is the macroscopic normal force applied during the rubbing process and b is the width of the substrate being rubbed. In roller rubbing, clearly the rubbing force varies across ℓ from low values at the leading and trailing edges, passing through a maximum where the pile deformation is a maximum. Thus a well-defined average value for F_f cannot be expected, but rather a

value which represents a range of forces across the majority of the contacted area. Assuming simple elastic deformation, with fibre force varying in proportion to the local pile deformation across ℓ, and neglecting interactions between fibres, the maximum force (F_{max}) will be 53% greater than the average value (F_f), and the force will be between $F_f/2$ and F_{max} over 80% of the distance ℓ. If the distribution of F across ℓ is flatter than in the simple elastic deformation model, or if all fibres do not make surface contact at all positions, then F_f as defined by equation (3) will be an underestimate.

If the average width of the microscopic fibre-surface contact w_f is known, then the rubbing ratio RR can be estimated from:

$$RR = w_f n_f \qquad (4)$$

Since w_f cannot readily be directly measured, it must be inferred from careful interpretation of rubbing-induced topographic features in AFM images.

Alignment layers were prepared using polyamide imide Probimide 32 (PI32, Ciba-Geigy Ltd.) and polyimide AL5417 (Japan Synthetic Rubber Co.). Films of 20–60 nm nominal thickness were spun down onto polished glass plates coated with indium tin oxide (ITO), and cured at the manufacturer's recommended bake temperature (170–300°C). Rubbing was performed using a 100 mm diameter roller covered with rayon cloth pressed down onto the plates so as to give a constant drum motor torque, corresponding with constant friction force. The rayon cloth pile was approximately 1 mm deep, and the maximum pile deformation during rubbing was approximately 0·3 mm, giving a roller contact length $\ell = 11$ mm. The normal force (F_N) and lateral force during rubbing of a 150 mm square plate coated with PI32 under the standard rubbing conditions were determined to be approximately 5·5 N and 3·0 N, respectively, giving a dynamic friction coefficient μ of 0·54. μ decreased from 0·58 to 0·53 as F_N was increased from 2 to 7 N. Layers were prepared with $v = 120$ rpm, giving a relative fibre-surface velocity v of 0·6 m s^{-1}, and with $N = 2$ and 6, giving rubbing lengths L of 500 mm and 1500 mm, respectively. Alignment layers prepared with $L =$ 1500 mm gave strong and uniform azimuthal anchoring (estimated azimuthal anchoring energy W_ϕ in excess of 10^{-4} J m^{-2}) and pretilt values of 2–4° measured for LC cells filled with nematic mixture E7 (Merck UK Ltd.) by the crystal rotation method [15] at room temperature.

The number of fibres per unit area of rubbing cloth σ_f was obtained from large area field emission scanning electron microscopy (SEM) images of the rubbing cloth used. Values of σ_f varied in the range 150–300 mm^{-2} at different positions. Therefore, from equation (2) n_f is 0·22–0·45 nm^{-1}, and on average one fibre every 2–4·5 nm passes across the substrate surface during the rubbing process. From equation (3), F_f is 11–22 μN. Close-up SEM images of the fibre terminations, such as in figure 1, showed the fibres, of overall diameter 10–20 μm, to have crenellated cross-sections with individual ridges of 2–5 μm diameter.

Rubbing-induced topographic features observed by tapping mode AFM (Nanoscope III or Dimension 3000 AFM, Digital Instruments Corp., USA) on AL5417 and PI32, have been described in detail previously [10]. The features include (a) occasional deep scratches of >5 nm peak-to-valley height and approximately 10 μm average spacing, (b) a high density of shallow scratches (depth < 2 nm, and mostly < 1 nm), and (c) in the case of AL5417, but not PI32, $>10^9$ cm^{-2} nanoscale surface islands (nanoislands) attributed to the balling up of loose polymer chains created during surface shearing. A particularly striking feature on the less strongly rubbed polymers (with $L = 500$ mm) was the quasi-periodic arrangement of nanoislands in the case of AL5417, and of background texture in the case of PI32. This effect is clear from the AFM images in figure 2. From this observation it was concluded that initial rubbing takes place by a stick–slip mechanism, with the slip phase involving balling of the nanoislands in the case of AL5417. Subsequent rubbing contact of regions with quasi-periodic features results in a tendency to randomise their distribution.

Since the number density of deeper scratches is such a small fraction of n_f (<1 in 1000), these must be defect-related features. This is consistent with their origin from relatively hard and sharp asperities, such as foreign material embedded in or trapped by the rubbing fibres. Thus w_f cannot be estimated from these deeper scratch marks. The number density of shallow scratches, with

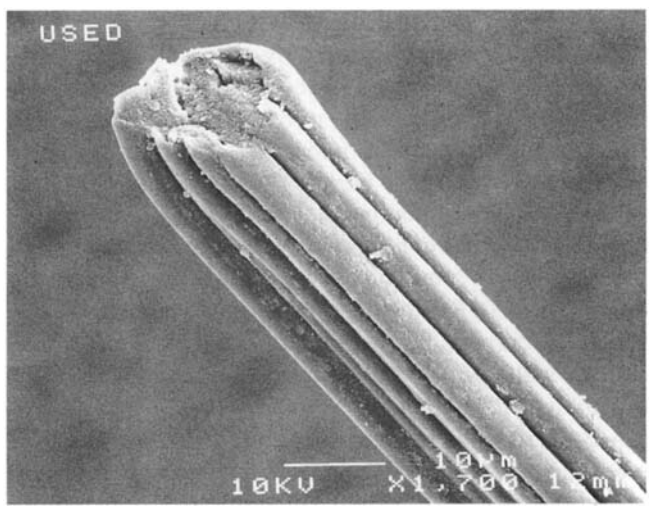

Figure 1. SEM micrograph showing the termination of a rubbing fibre after use.

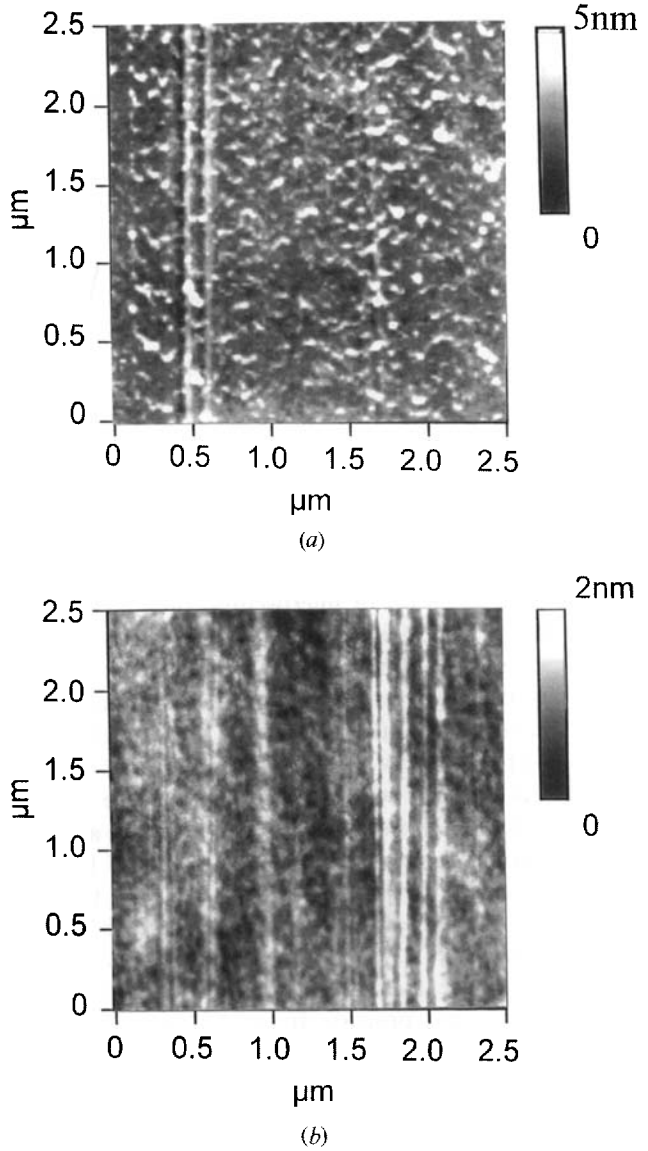

Figure 2. 2·5 μ-square AFM images from rubbed (*a*) AL5417 and (*b*) PI32 after $L = 500$ mm; the rubbing direction is vertical in each case.

widths of 10–50 nm, at a maximum of $10\,\mu m^{-1}$ after $L = 500$ mm, is still small compared with $n_f = 75$–$150\,\mu m^{-1}$, suggesting that these also may not form the majority contact.

The relatively uniform surface coverage by nanoislands in the case of AL5417, and by background marks in the case of PI32, even after $L = 500$ mm, suggests that it is more appropriate to base estimates of average contact areas on these features. Their widths after the first pass by a fibre may provide a measure of w_f. Subsequent passes will cause features to overlap and, in the case of nanoislands, a tendency for them to be moved together, swept up or squeezed outwards from the contact. Feature widths after partial rubbing ($L = 500$ mm) were frequently in the range 100–300 nm, and occasionally about 500 nm. The period of nanoislands on AL5417 and background marks on PI32 may likewise provide an upper estimate of the length of the fibre–surface contact, as the fibre slips to its next position leaving the mark or nanoisland behind. Typical periods of 100–200 nm were observed. Similar widths and lengths of the contacts might be expected if fibre terminations were the main contact point with the surface.

AFM feature widths relate to the width over which surface plastic deformation has occurred. They may give an overestimate of the true fibre–surface contact width w_f due to plastic deformation occurring around the contact zone (see figure 3), or lateral movement of nanoparticles after formation. We therefore take a value of 100 nm, at the lower end of the range of quasi-periodic feature widths, as a conservative estimate of w_f. This leads to $RR = 7{\cdot}5$–15 after $L = 1500$ mm. It is not surprising from this that a conclusion from the topographic study [10] was that the entire alignment polymer surface had been modified during the rubbing process.

Figure 3 shows a schematic of the isolated fibre–surface interaction. The alignment layer surface experiences a travelling microscopic shear stress pulse, with a tendency to produce in-plane compression ahead of the contact and tension behind it. The fibre surface experiences an opposite shear stress, modulated at the frequency of stick–slip, if this is occurring. The extent of resulting elastic and plastic deformation depends on the materials involved and on the stresses, stress rates and temperatures occurring in and around the contact zone, which we will now briefly consider. It is proposed that plastic deformation by shear yielding produces, by a

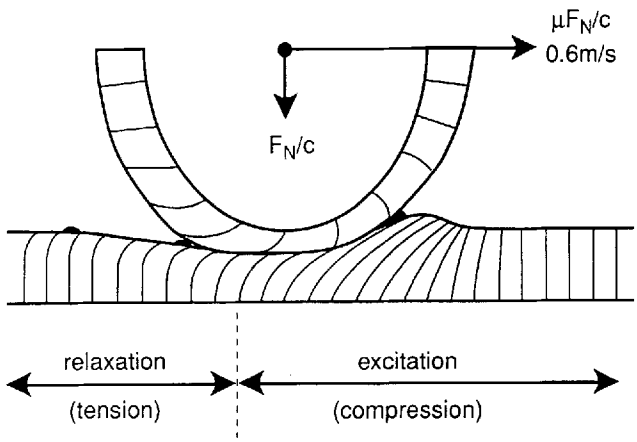

Figure 3. Schematic illustration showing the deformation around a fibre–surface microscopic mechanical contact region under an applied normal force F_N/c at a velocity $v = 0{\cdot}6\,m\,s^{-1}$.

process resembling cold drawing, the polymer chain orientation believed responsible for LC alignment [16].

The normal pressure and shear stress within the fibre–surface contact zone are given approximately by $4F_f/\pi c w_f^2$ and $4\mu F_f/cw_f^2$, respectively, where c is the average number of surface contacts per fibre. Assuming that 1 or 2 contacts per fibre are probable and values of 0 or >2 less probable, gives shear stresses of 0·4–1·5 GPa with $w_f = 100$ nm. Given the range of AFM feature widths (10–500 nm), this can be taken as only a mid-range estimate of actual contact stresses. The true values will furthermore fluctuate with position across the contact zone, since the larger contact areas may comprise several nano-asperity contacts, and also with time as a consequence of stick–slip motion. Since surface plastic deformation is clearly occurring across the contact width, the normal and shear contact stresses given above may be equated with the yield stress (Y) and critical shear stress (S), respectively, under the conditions of rubbing. The range of S estimated exceeds the values of $\leqslant 0{\cdot}06$ GPa reported for many polymers at slow sliding speeds [17]. The difference reflects the viscoelastic nature of polymers, and the much reduced opportunity for plastic flow at the high rubbing velocity v. At $v = 0{\cdot}6\ \mathrm{m\,s^{-1}}$, the contact length corresponds to a pressure pulse with a peak duration of $\sim 0{\cdot}2\ \mu$s. This indicates that w_f could be largely determined by the mechanical response at MHz frequencies, where high elastic moduli and low viscous energy loss are expected. A Hertzian model of sphere–flat contact predicts an elastic contact radius given by $(3F_f R/4cE)^{1/3}$, where R is the sphere radius and E the Young's moduli of the materials involved. Taking $R = 1$–$2{\cdot}5\ \mu$m (the radius of fibre crenellations) and $E = 2$–11 GPa as a range typical of stiffer polymers [18] gives elastic contact diameters of 150–500 nm, comparable with AFM quasi-periodic feature widths.

The contact temperature rise (T_c) above the rubbing temperature (room temperature) has been estimated by Mada and Sonoda [19] using a simple heat-flow model outlined by Harper [20]. T_c is approximately given by $\pi r_h \mu v Y/4(k_1 + k_2)$, where r_h is the radius of contacted hot-spot and $k_1(k_2)$ are the alignment polymer (fibre) thermal conductivities. Equating r_h with $w_f/2$, T_c values of 45–180 K are predicted with $Y = 0{\cdot}7$–$2{\cdot}8$ GPa (i.e. $w_f = 100$ nm) and $k_1 = k_2 = 0{\cdot}1\ \mathrm{J\,m^{-1}s^{-1}K^{-1}}$. This T_c range, which is subject to considerable uncertainties, compares with a value of 230 K obtained by Mada and Sonoda using very different values of Y and v. Our estimated contact temperatures are lower than glass transition temperatures, T_g, reported for alignment polymides, which may exceed 300°C [21, 22]. However, many glassy polymers remain ductile below their T_g, especially under high compressive stress which, as figure 3 shows, occurs both ahead of and beneath the fibre contact. Furthermore, much of the polymer alignment is known to take place in the top few nm of the film [21, 22] where the polymer structure and impurity levels may differ substantially from the bulk. Significant lowering of T_g has been measured in ultra-thin polymer films [23], indicating enhanced near-surface mobility and ease of molecular reorientation. For these reasons, near-surface orientation of polymer chain segments may occur even if temperatures are well below the bulk T_g. Surface chain alignment may occur both within the contact zone and in the near-surface region immediately around this where the polymer is under shear or tension, relatively unconstrained, and remains warm for a transient period. Triboelectric effects, due to electronic excitation by high fields established across the contact, may also play a role [20].

In conclusion, we have used macroscopic measurements of the rubbing process mechanics, in conjunction with an interpretation of microscopic rubbing-induced surface topographic features, to estimate micromechanical properties of the fibre–surface contact. The necessarily simplistic analysis treats cloth fibres as isolated and assumes most, if not all, contact the surface at 1 or 2 points. The results show that a mild macroscopic rubbing pressure ($\sim 3{\cdot}3$ kPa), when transmitted to the surface through individual fibre points of contact, belies aggressive microscopic contact pressures estimated to be near the GPa range. It is confirmed that the thermo-viscoelastic properties of near-surface regions of the polymer film and rubbing fibres, as well as of any intervening surface layer, are critical to an understanding of the microscopic process. It is also estimated that during our standard rubbing conditions, the entire surface may have been contacted approximately 10 times. Both this degree of over-rubbing, and the surface contact forces in use, may exceed the mechanical conditions strictly necessary to effect polymer surface alignment. The incidence of rubbing-induced defects can be lowered if the harshness of the rubbing treatment can be minimised without reducing its effectiveness.

The authors are indebted to C. Reeves for SEM imaging, and to I.C. Sage, S. Cunningham and K. Blackwood for helpful discussions. This work was supported by EC ESPRIT II programme ECAMII (AMAT work package).

References

[1] Raynes, E. P., 1978, U.S. Patent 4,084,884.
[2] Castellano, J. A. 1983, *Mol. Cryst. liq. Cryst.*, **94,** 33.
[3] Becker, M. E., Kilian, R. A., Kosmowski, B. B., and Mlynski, D. A., 1986, *Mol. Cryst. liq. Cryst.*, **132,** 167.
[4] Uchida, T., Hirano, M., and Sakai, H., 1989, *Liq. Cryst.*, **5,** 1127.

[5] KADO, H., YOKOHAMA, K., and TOHDA, T. 1992, *Rev. Sci. Instrum.*, **63,** 3330.
[6] LEE, E. S., SAITO, Y., and UCHIDA, T., 1993, *Jpn. J. appl. Phys.*, **32,** L1822.
[7] SEO, D-S., OH-IDE, T., MATSUDA, H., ISOGAMI, T-R., MUROI, K-I., YABE, Y., and KOBAYASHI, S. 1993, *Mol. Cryst. liq. Cryst.*, **231,** 95.
[8] ZHU, Y-M., WANG, L., LU, Z-H., WEI, Y., CHEN, X. X., and TANG, J. H., 1994, *Appl. Phys. Lett.*, **65,** 49.
[9] KIM, Y. B., OLIN, H., PARK, S. Y., CHOI, J. W., KOMITOV, L., MATUSZCZYK, M., and LAGERWALL, S. T., 1995, *Appl. Phys. Lett.*, **66,** 2218.
[10] PIDDUCK, A. J., BRYAN-BROWN, G. P., HASLAM, S. D., BANNISTER, R., KITELY, I., MCMASTER, T. J., and BOOGAARD, L., 1996, *J. Vac. Sci. Tech.*, **A14,** 1723.
[11] HUANG, J. Y., LI, J. S., JUANG, Y.-S., and CHEN, S.-H. 1995, *Jpn. J. appl. Phys.*, **34,** 3163.
[12] ITO, T., NAKANISHI, K., NISHIKAWA, M., YOKOYAMA, Y., and TAKEUCHI, Y., 1995, *Polym. J.*, **27,** 240.
[13] VAN AERLE, N. A. J. M., 1994, *J. S.I.D.* **2,** 41.
[14] SEO, D-S., MUROI, K-I., and KOBAYASHI, S., 1992, *Mol. Cryst. liq. Cryst.*, **213,** 223.
[15] BAUR, G., WITTWER, V., and BERREMAN, D. W., 1976, *Appl. Phys. Lett.*, **56A,** 142.
[16] GEARY, J. M., GOODBY, J. W., KMETZ, A. R., and PATEL, J. S., 1987, *J. appl. Phys.*, **62,** 4100.
[17] BOWDEN, F. P., and TABOR, D., 1964, *The Friction and Lubrication of Solids*, Part II, (Oxford: Clarendon Press), Chap. XIII.
[18] ROFF, W. J., 1956, *Fibres, Rubber and Plastics* (Butterworths: London).
[19] MADA, H., and SONODA, T., 1993, *Jpn. J. appl. Phys.*, **32,** L1245.
[20] HARPER, W. R., 1967, *Contact and Frictional Electrification*, (Oxford: Clarendon Press).
[21] VAN AERLE, N. A. J. M., and TOL, A. J. W., 1994, *Macromolecules*, **27,** 6520.
[22] TONEY, M. F., RUSSELL, T. P., LOGAN, J. A., KIKUCHI, H., SANDS, J. M., AND KUMAR, S., 1995, *Nature*, **374,** 709.
[23] KEDDIE, J. L., and JONES, R. A. L., 1995, *Isr. J. Chem.*, **35,** 21.